NUMERICAL DETERMINATION OF LIBRATION POINT TRAJECTORIES WITH OUT-OF-PLANE MANEUVERS TO AVOID THE SOLAR EXCLUSION ZONE

Henry J. Pernicka[1] and Kathleen C. Howell[2]

Three-dimensional orbits in the restricted three-body problem have been the subject of a number of recent studies. One type of three-dimensional, quasi-periodic orbit that emanates from the general vicinity of the collinear libration points is known as a "Lissajous" trajectory. Future mission plans include trajectories near the interior libration point (L_1) in the Sun-Earth system and may employ Lissajous orbits as part of the trajectory design. Such orbits may be constrained, however, to remain beyond the region of the solar disk as viewed from Earth. This effort involves the numerical determination of Lissajous trajectories of arbitrary, but predetermined, length that never violate such a constraint by use of maneuvers directed, in general, perpendicular to the ecliptic plane.

INTRODUCTION

Current interest in spacecraft trajectories near L_1, the interior libration point of the Sun-Earth system, has created a need for accurate trajectory determination methods for orbits in this vicinity. In the restricted three-body problem, a particular type of bounded, three-dimensional solution associated with the collinear libration points has been studied by a number of authors. Farquhar and Kamel[1] used the method of Linstedt-Poincaré to produce a third-order analytic solution for such orbits near the translunar libration point (L_2) of the Earth-Moon system. Richardson and Cary[2] also developed a series solution, truncated to fourth order, for orbits near L_1 or L_2 in a Sun-Earth system. These analytic approaches describe the bounded motion, in part, in terms of a set of three amplitudes. Each amplitude provides an approximate bound on the distance the satellite moves in one of the three spatial dimensions. The series solutions show that for motion with small amplitudes relative to the libration point, the orbital path traces out a Lissajous figure (when viewed by an observer on either primary). These paths of motion are thus termed "Lissajous" trajectories. When the amplitudes are sufficiently large, nonlinear terms may be used to compute constraint relationships between the amplitudes that result in three-dimensional, periodic paths sometimes called "halo" orbits. They appear in any planar projection as generally elliptical in shape.

---

1 Graduate Student, School of Aeronautics and Astronautics, Purdue University, West Lafayette, IN 47907.

2 Associate Professor, School of Aeronautics and Astronautics, Purdue University, West Lafayette, IN 47907.

AAS 89-172-1

When mission planning requires trajectories of smaller amplitudes, for which halo orbits fail to exist, Lissajous orbits may be a remaining option. While Lissajous trajectories have been computed analytically from the series solutions, numeric computations have been limited due to their non-periodicity. Howell and Pernicka[3] have developed a technique for the numerical determination of Lissajous orbits in the circular restricted three-body problem that produces a numerically integrated path of arbitrary length. The method has since been extended for use in the elliptic problem[4], as well as with a dynamic model using ephemeris data (represented in terms of polynomial functions) to locate the positions of the Sun, Earth, and Moon[5].

There is, however, an inherent difficulty with using Lissajous trajectories for certain missions. For example, spacecraft orbits near L_1 in the Sun-Earth system must remain sufficiently far from the Sun-Earth line to avoid crossing the solar disk (as seen from Earth) so that communications are not disrupted by the intense solar activity. Difficulties meeting this constraint arise because spacecraft in Lissajous trajectories will occasionally pass into this region if the orbit is allowed to evolve naturally. The objective of this work was to numerically compute velocity maneuvers that alter the "natural evolution" of the path such that the solar disk constraint is satisfied for the entire mission. More specifically, the maneuvers are computed such that the shape of the orbit can be somewhat controlled. The original motivation for this study was to determine nominal paths for possible future missions that may include motion in the vicinity of the Sun-Earth L_1 point and may consider the use of Lissajous trajectories. Therefore, the examples that are discussed all correspond to the Sun-Earth/Moon barycenter system and include orbital parameters consistent with possible trajectories for a particular mission. The methods, however, apply equally well to other systems and are also applicable to the L_2 libration point.

BACKGROUND

Equations of Motion

Two dynamic models are used to derive two different sets of equations governing motion in this problem. First, in order to gain an initial understanding into the problem, the equations of motion associated with the elliptic restricted three-body problem (referred to here as the ER3BP) are used. Once the techniques are successfully developed using the ER3BP model, a second model is used which obtains the locations of the Sun and Moon relative to the Earth from a polynomial representation of ephemeris data. In this manner, the methods developed can be tested in a model in which the primary motion is no longer periodic. This latter model is termed the "Sun-Earth-Moon model", abbreviated here as the "SEM model".

In developing the equations of motion associated with the ER3BP, the usual rotating coordinate frame is used in which the x-axis is directed from the larger to the smaller primary. The y-axis is 90° from the x-axis in the primaries' plane of motion. The z-axis completes the right-handed system, defining the out-of-plane direction. The associated unit vectors are denoted $\hat{x}$, $\hat{y}$, $\hat{z}$ respectively. The problem is nondimensionalized in the usual way and the nondimensional mass of the smaller primary is represented as μ.

Let the vector $\bar{\rho}$ describe the nondimensional position of the infinitesimal mass with respect to the center of mass of the primaries such that $\bar{\rho}$ has components x, y, and z. In the standard formulation of the ER3BP, then, the (nondimensional) equations of motion can be written in the form

$$\ddot{x} - 2n\dot{y} = \frac{\partial U}{\partial x} + \dot{n}y$$
$$\ddot{y} + 2n\dot{x} = \frac{\partial U}{\partial y} - \dot{n}x \qquad (1)$$
$$\ddot{z} = \frac{\partial U}{\partial z} ,$$

where

$$U = \frac{1}{2}n^2(x^2 + y^2) + \frac{(1-\mu)}{d} + \frac{\mu}{r} ,$$

and "d", "r" are distances of the satellite relative to the larger and smaller primary, respectively. Note that "n" represents the nondimensional angular velocity of the rotating frame and is time-varying due to orbital eccentricity. Dots indicate differentiation with respect to nondimensional time. Also needed is the 6 x 6 state transition matrix $\Phi(t,t_o)$, which is composed of the the partial derivatives $\partial X(t)/\partial X(t_o)$, where X is defined as the state and represented as a column vector with elements x, y, z, $\dot{x}$, $\dot{y}$, $\dot{z}$. As usual, $\Phi(t_o,t_o) = I$, where I is the identity matrix, and the matrix differential equation governing $\Phi(t,t_o)$ is written

$$\frac{d}{dt}\Phi(t,t_o) = A(t)\,\Phi(t,t_o) , \qquad (2)$$

where

$$A(t) = \begin{bmatrix} 0 & I \\ U_{xx} & 2n\Omega \end{bmatrix} , \quad \Omega = \begin{bmatrix} 0 & 1 & 0 \\ -1 & 0 & 0 \\ 0 & 0 & 0 \end{bmatrix} ,$$

and U_{xx} is the symmetric matrix of second partial derivatives of U with respect to x, y, z evaluated along the orbit.

In approaching the problem, it was required that any method developed not be dependent on the periodicity of the orbits of the primaries. Therefore, an additional model for primary motion was defined to represent the use of observational data for the locations of the bodies which exert forces on the spacecraft. Thus the "SEM model" has been developed that uses ephemeris data written in terms of polynomial functions to locate the Sun and Moon relative to the Earth. The model was not developed to include all perturbations on the spacecraft, nor to provide extremely accurate solar and lunar positions. Rather, it is used as a tool to provide an environment in which the analytical and numerical methods can be demonstrated. The SEM model, in its current form, assumes the only forces acting on the spacecraft are gravitational forces from the Sun, Earth, and Moon. Of course, it can be expanded to include additional force systems.

Lissajous Orbits

The equations of motion in Eq. (1) can be expanded about L_1 or L_2. Define translated position coordinates x,y,z relative to L_i Then the linearized form of the differential equations (1) about L_1 or L_2 appear as

$$\ddot{x} - 2\dot{y} - (1+2c)\,x = 0$$
$$\ddot{y} + 2\dot{x} + (c-1)\,y = 0 \qquad (3)$$
$$\ddot{z} + cz = 0 ,$$

where 'c' is a positive constant. The solution to Eq. (3) for the out-of-plane z motion is

simple harmonic. The characteristic equation for the in-plane $x-y$ motion has two real and two imaginary roots. If only the non-divergent modes are excited (by judicious selection of initial conditions), the solution is bounded and can be written in the form

$$\begin{aligned} x &= -kA_y \cos(\lambda t + \phi) \\ y &= A_y \sin(\lambda t + \phi) \\ z &= A_z \sin(\nu t + \psi) \,. \end{aligned} \tag{4}$$

The linearized solution is then characterized by the two amplitudes A_y and A_z, and the two phase angles ϕ and ψ. When the frequencies λ and ν are equal, a halo orbit results which repeats with every revolution. The more general case of unequal frequencies yields Lissajous trajectories that do not quite repeat after each revolution.

The higher order approximations of motion relative to L_i use Eq. (4) as the first term and are written as functions of A_y, A_z, ϕ, and ψ. Because the original focus of this study was to determine libration point trajectories in the Sun-Earth system, the solution developed by Richardson and Cary[2] is used primarily. Their solution is actually written for the lunar perturbed Sun-Earth system, in which the primaries in the "three-body" system are the Sun and the Earth/Moon barycenter. Using this system provides a better approximation to the problem as shown by Farquhar[6]. The methods of dual time scales and successive approximations are employed to develop a fourth-order expansion including corrections for the Earth/Moon mass ratio, and the eccentricity of the path of the Earth/Moon barycenter about the Sun. The result is applicable to orbits associated with the interior libration point L_1, as well as L_2. Development of the higher order terms is given in detail in the reference.

One method for the numerical determination of Lissajous trajectories is given by Howell and Pernicka[3], with further developments in references 4 and 5. Their method seeks a continuous, bounded path as a result of the (numerical) integration of the exact equations of motion. The technique, a two-level iteration process, has been used to successfully compute Lissajous trajectories numerically for an arbitrary number of revolutions using either the ER3BP or the SEM model. The approach first identifies target positions at specified intervals along the trajectory. The six-dimensional state (position and velocity) at each point is initially defined from an approximate analytic solution or from a continuation algorithm. Trajectory segments between the targets are joined in an iterative manner such that the Lissajous path is continuous in position with an arbitrary but predetermined number of velocity discontinuities ($\Delta\bar{v}$'s) at the target points. This process is defined as the first level iteration. The $\Delta\bar{v}$'s are then simultaneously reduced in a second level iteration process which "corrects" the positions of the targets. When the first level iteration sequence is repeated, the $\Delta\bar{v}$'s are significantly decreased. Both iteration processes use a differential corrections scheme, and five iteration sets (levels one and two) are usually sufficient to bring all the $\Delta\bar{v}$'s to an acceptably small magnitude. The result is a numerically integrated Lissajous orbit continuous in position and velocity, suitable for use as a nominal path.

Fig. 1 shows three planar projections of a Lissajous trajectory associated with the L_1 libration point of the Sun-Earth/Moon barycenter system. In the figure, the origin in each plot corresponds to L_1. The orbit was numerically computed with the SEM model using the approximate solution of Richardson and Cary through third order, including eccentric effects, to provide the initial guess. The amplitudes and phase angles required as inputs to produce the approximate solution were specified as $A_y = A_z = 157{,}000$ km, $\phi = 14.9°$, and $\psi = -26.4°$. The trajectory has a duration of 6.69 years. Note that solutions can be produced for any combination of inputs and the amplitudes need not be equal. These particular input parameters were selected to correspond to a mission plan

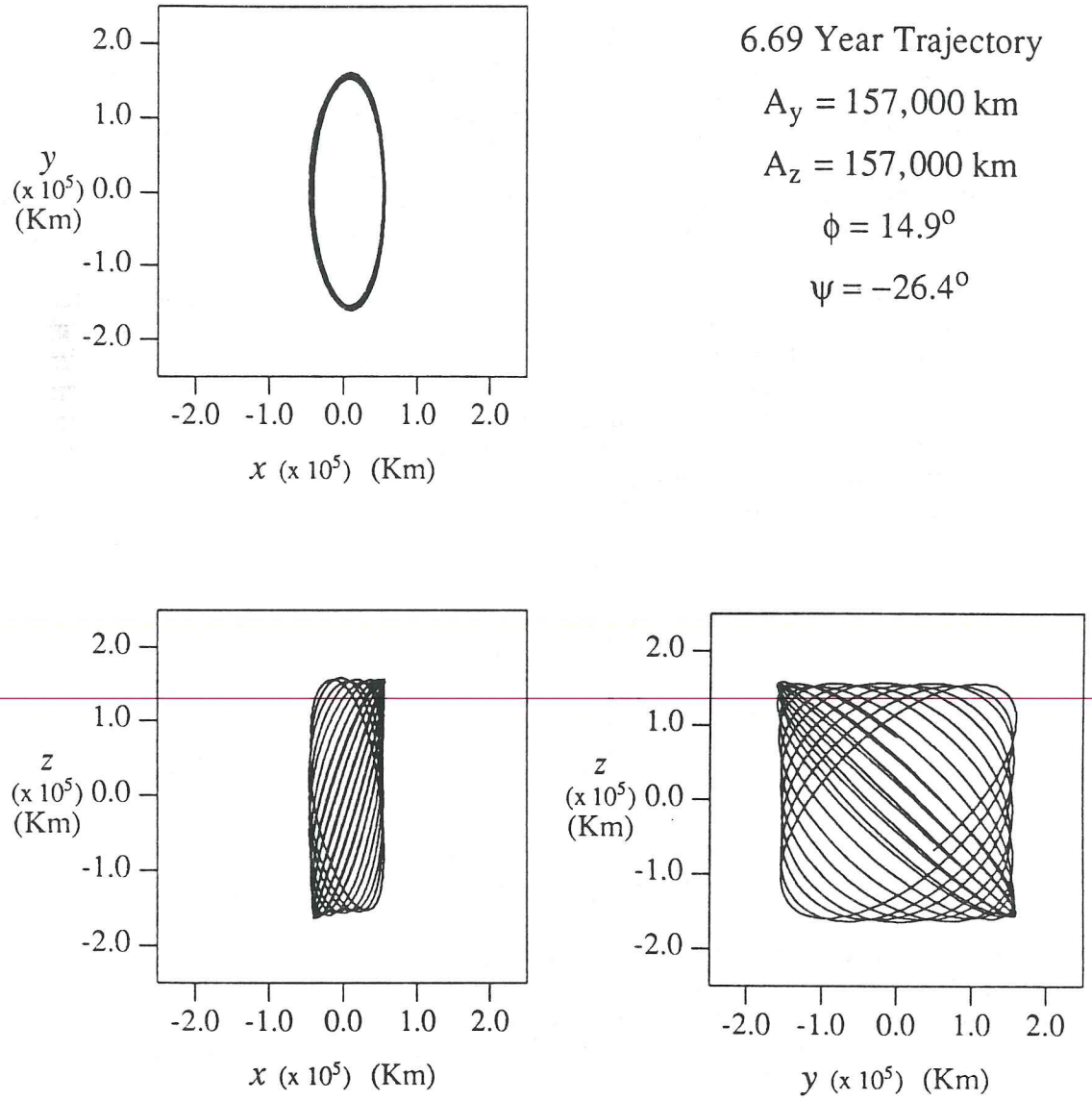

Fig. 1 Example of Numeric Solution Using SEM Model

that was considered for the Solar and Heliospheric Observatory (SOHO) spacecraft, currently scheduled for launch in 1995.

TRAJECTORY DESIGN TO AVOID THE SOLAR EXCLUSION ZONE

Definition of the Solar Exclusion Zone

There are currently a number of missions in the planning stage that might result in the placement of spacecraft in Lissajous-type trajectories in the L_1 neighborhood of the Sun-Earth/Moon barycenter system. A satellite in such an orbit will periodically cross in front of the solar disk when viewed from Earth. Mission constraints may be defined to insure that the spacecraft will remain sufficiently far from the solar disk to prevent the disruption of communications. In this analysis, such constraints are represented in the form of an angle that defines a radial distance D perpendicular to the Sun-Earth/Moon barycenter line ($\hat{x}$ axis) at the libration point L_1. Motion is then assumed to be constrained to remain beyond this distance from the $\hat{x}$ axis at all times, even when the vehicle moves slightly nearer or further from the Earth than L_1. Fig. 2 shows the geometry involved, assuming elliptic primary motion, with β representing the constraint angle. The distance D then provides an inner limit for spacecraft motion, i.e., how close the spacecraft may approach the Sun-Earth/Moon barycenter line. D can be easily computed if the distance between the Earth/Moon barycenter and the libration point is known, using the relationship $D = R\,\gamma_L \tan\beta$, where R is the distance between the Sun and Earth/Moon barycenter, and γ_L is the constant ratio of the distances Earth/Moon barycenter-L_1 to R.

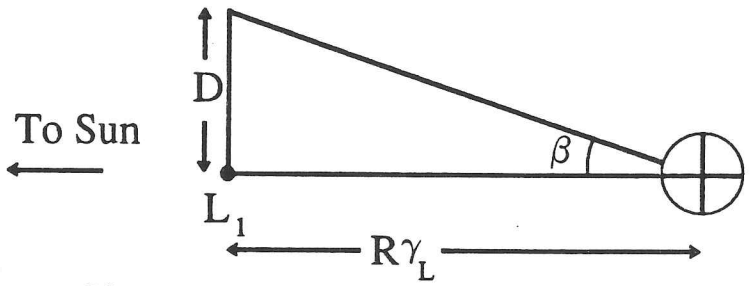

Fig. 2 Definition of the Solar Exclusion Zone

Since the x–component of the spacecraft position relative to Earth varies slightly around L_1, the value of D can be considered as the radius of a short cylinder that defines the solar exclusion zone from which the path of the spacecraft must be excluded. In addition, due to the eccentricity in the primary system, R will vary with time causing D to change depending on the instantaneous location of the primaries. As the primaries move in their respective orbits, the cylindrical radius actually "oscillates" slightly in size between its minimum and maximum value. The constant value of D used in this analysis corresponds to the maximum or "worst case" radius.

Selection of Phase Angles

The numerical algorithm using the approach by Howell and Pernicka for computing Lissajous trajectories requires an initial approximation for the orbit of interest. Typically, an analytic approximation is used that includes some higher order effects. The two input phase angles required by an analytic solution determine the location along the Lissajous curve at which the trajectory originates. A method was sought that would select both phase angles such that the ensuing trajectory avoids the exclusion zone for the

maximum length of time, thus reducing the number of design maneuvers required to prevent violation of the zonal constraint.

The most useful approach for the orbit sizes of interest defines a cost function from the linearized solution. It can then be used to maximize the length of time that the linear solution (trajectory path) remains outside the exclusion zone. In particular, define a cost function f_o as

$$f_o(t) = y^2 + z^2, \tag{5}$$

that represents the square of the radial distance from the libration point (in the $y-z$ plane), where y and z are the linear solutions defined by Eq. (4). Then an optimization problem is defined, whereby, given some time $t_d > 0$,

$$V(t_d) = \int_0^{t_d} f_o(t)\, dt \tag{6}$$

is to be maximized over all choices of ϕ and ψ. Let ϕ^* and ψ^* represent the stationary points corresponding to Eq. (6) for ϕ and ψ, respectively. These algebraic relationships yield

$$\phi^* = \frac{1}{2}\tan^{-1}\left[\frac{\cos(2\lambda t_d)-1}{\sin(2\lambda t_d)}\right], \quad \psi^* = \frac{1}{2}\tan^{-1}\left[\frac{\cos(2\nu t_d)-1}{\sin(2\nu t_d)}\right]. \tag{7}$$

Thus, the optimal phase angles are functions of linearized frequencies λ and ν, as well as the duration of the trajectory, i.e., t_d. It is noted that Eq. (7) provides two values for each ϕ^* and ψ^*, since the inverse tangent function can be taken in either of two quadrants. Thus there are four possible combinations of angle pairs ϕ^* and ψ^*. Two of the pairs maximize Eq. (6), while the other pairs minimize Eq. (6). In practice, the desired values for ϕ^* and ψ^* that maximize Eq. (6) are readily apparent.

Fig. 3 shows an example of a Lissajous trajectory in the Sun-Earth/Moon barycenter system that is generated from the third order analytic solution of Richardson and Cary (including eccentric effects through third order) using optimal phase angles obtained from Eq. (7). The figure shows the $y-z$ projection of the orbit, and also includes a circle

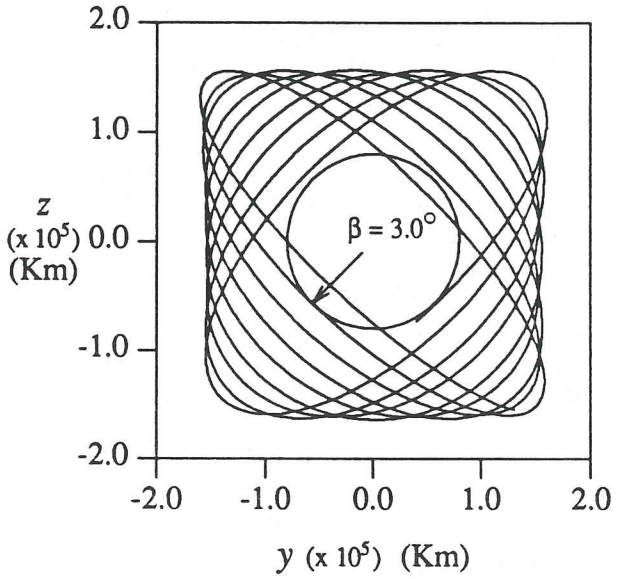

Fig. 3 Example of Third Order Analytic Solution

AAS 89-172-7

representing an inner constraint of $\beta = 3.0^\circ$. When computing ϕ^* and ψ^*, t_d was (iteratively) chosen such that the trajectory begins just outside of the inner constraint. Then t_d is the approximate maximum time the satellite may remain outside the exclusion zone without use of maneuvers. In the figure, however, the trajectory is allowed to proceed beyond t_d in order to demonstrate that the path will eventually violate the inner constraint.

Out-of-Plane Maneuvers to Avoid Exclusion Zone

Z-Axis Control Strategy. Even when using optimal phase angles, the duration of some missions may result in trajectories which violate the exclusion zone, as Fig. 3 demonstrates. Although excursions into the exclusion zone may be minimized, *any* violation may be deemed unacceptable. In such cases, out-of-plane maneuvers can be computed which will allow the spacecraft to remain at an acceptable distance beyond the inner constraint. Use of "z-axis control" first appeared in the late 1960's, with publications from the General Electric Company[7], R.W. Farquhar[8–10], and T.A. Heppenheimer[11]. All of these analyses were performed using the linearized approximations shown in Eq. (4) for a Lissajous trajectory, and they assumed that the maneuvers were to be applied in the out-of-plane or "z" direction. Performing the maneuvers in the out-of-plane direction is not necessarily the optimal solution, but it does provide a method that succeeds in preventing the satellite from entering the exclusion zone.

As is standard for Lissajous shapes, when the in-plane and out-of-plane frequencies in Eq. (4) are slightly different, the resulting path in the $y-z$ projection does not repeat with every revolution, as shown in Fig. 3. This projection can be considered as being comprised of a series of revolutions, each one generally elliptical in shape, that continually "evolve" along the trajectory. For phase angles determined by Eq. (7), the initial point on the trajectory is selected such that the first revolution just "skims" the edge of the exclusion zone. An approach to incorporate the z-axis control plan is to let the Lissajous curve then develop naturally until its path evolves into a near-circular shape. The z-axis control strategy is then employed for a predetermined number of revolutions to maintain the near-circular shape. Finally, the z-axis control is discontinued and the trajectory returns to its natural evolutionary path. In this manner, the $\Delta\bar{v}$ costs can be reduced by taking advantage of the "cost-free" portion of the Lissajous orbit that remains outside of the exclusion zone. This, then, is the overall approach to avoiding the solar exclusion zone for a trajectory of any specified size and length. The details for determining an approximate path and the corresponding $\Delta\bar{v}$'s are given below.

Linear Analysis for Z-Axis Control. One method for using z-axis control to avoid the exclusion zone proceeds as follows, with references [7-11] as a guide. The concept of z-axis control uses planned maneuvers in the z-direction in order to reduce the period of the out-of-plane z-motion to match that of the in-plane $(x-y)$ motion (note that the "z" and "z" directions are identical). If this is done for a portion of the Lissajous path that misses the excluded zone, then this near-circular path can be repeated indefinitely by executing the z-directional maneuvers at the appropriate times. To determine the out-of-plane maneuvers, consider the following.

If the last equation of Eq. (4) is differentiated with respect to time, then the spacecraft velocity in the z-direction is written

$$\dot{z}(t) = A_z \nu \cos(\nu t + \psi) . \tag{8}$$

Squaring Eqs. (4) and (8) and adding the result yields

$$z^2 + (\dot{z}/\nu)^2 = A_z^2 \,. \tag{9}$$

Fig. 4 shows the resulting phase-plane trajectory resulting from Eq. (9) for the linearized motion in the z-direction. The path is circular with radius A_z, and proceeds in a clockwise direction. One complete rotation corresponds to approximately one revolution about the libration point, and this time period is defined as $\mathbf{P}_z$. The period of the corresponding $x-y$ motion is defined as $\mathbf{P}_{xy}$, and is typically shorter in duration than $\mathbf{P}_z$. The difference between the two periods is thus defined

$$\Delta\mathbf{P} = \mathbf{P}_z - \mathbf{P}_{xy} \,, \tag{10}$$

where

$$\mathbf{P}_z = 2\pi/\nu \,, \quad \mathbf{P}_{xy} = 2\pi/\lambda \,. \tag{11}$$

In the phase-plane plot, an angle of rotation, θ, is defined as

$$\theta(t) = \nu t + \psi \,, \tag{12}$$

and is measured positive clockwise from the vertical $(\dot{z}/\nu)$ axis.

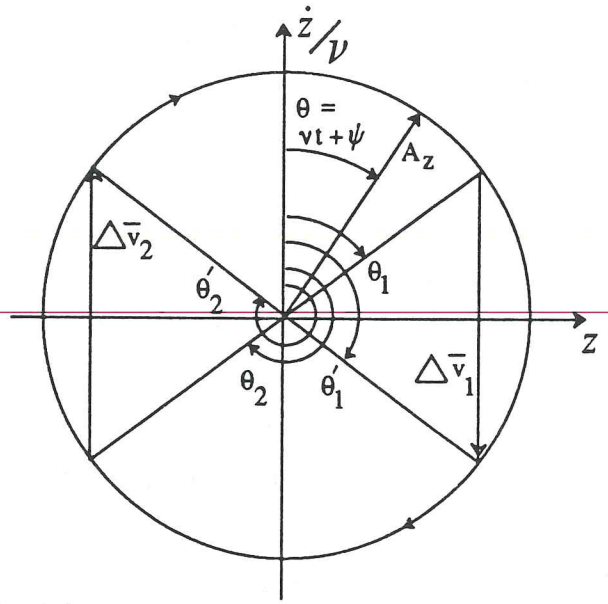

Fig. 4 Phase-Plane Plot of Out-of-Plane Motion

A method to reduce the value of the z-period to correspond to that of the xy-period is outlined in Fig. 4. Two delta-V's ($\Delta\bar{v}$'s) per revolution are implemented, one near the maximum z-excursion point and the other near the point of minimum z-excursion. In this manner, a portion of the z-motion is "trimmed", thus reducing the z-period. As shown in the figure, the first $\Delta\bar{v}$ is executed at $\theta = \theta_1$, with the effect of "moving" the spacecraft (instantaneously) to θ_1 on the figure. Also defined are times t_1 and t_1', corresponding to locations on the original path at θ_1 and θ_1', respectively. Similar definitions apply for the second $\Delta\bar{v}$. So $(t_1' - t_1)$ reflects the amount of time "trimmed" from the original period by the maneuver $\Delta\bar{v}_1$. Thus, in order to reduce $\mathbf{P}_z$ by the required amount in Eq. (10), the relationship

$$\delta\mathbf{P}_z = -\Delta\mathbf{P} = -(t_1' - t_1) - (t_2' - t_2) \tag{13}$$

must be satisfied. If $t_1' - t_1$ is defined as Δt_1, and by defining Δt_2 similarly, Eq. (13) can

be written as

$$\delta P_z = -(\Delta t_1 + \Delta t_2) . \tag{14}$$

Using the geometry of Fig. 4, the $\Delta\bar{v}$ cost per revolution can be expressed as

$$|\Delta\bar{v}_1| + |\Delta\bar{v}_2| = 2 A_z \nu \left[\left| \sin\left[(\theta_1' - \theta_1)/2\right] \right| + \left| \sin\left[(\theta_2' - \theta_2)/2\right] \right| \right]$$

$$= 2 A_z \nu \left[\left| \sin(\nu\Delta t_1/2) \right| + \left| \sin(\nu\Delta t_2/2) \right| \right] . \tag{15}$$

In order to minimize $\Delta\bar{v}$ expenditure, a cost function is obtained from Eq. (15) by enforcing the constraint in Eq. (14), resulting in

$$f_v(\Delta t_2) = \left| \sin\left[-\nu(\delta P_z + \Delta t_2)/2\right] \right| + \left| \sin(\nu\Delta t_2/2) \right| . \tag{16}$$

The stationary points corresponding to Eq. (16) are given by

$$\Delta t_2 = -\delta P/2 \pm 2n/\nu , \quad n = 0, 1, 2, ... \tag{17}$$

and thus the optimal value is

$$\Delta t_2^* = -\delta P/2 . \tag{18}$$

Substituting Eq. (18) into Eq. (14) yields the corresponding optimal value Δt_1^* as

$$\Delta t_1^* = -\delta P/2 . \tag{19}$$

To compute the $\Delta\bar{v}$ cost, first note that, for the optimal solution,

$$\theta_1' - \theta_1 = \theta_2' - \theta_2 = \nu\,\Delta t_1 . \tag{20}$$

Substituting Eq. (20) into Eq. (15) results in the $\Delta\bar{v}$ cost per revolution written as

$$|\Delta\bar{v}| = 4\,\nu\,A_z \sin(\nu\Delta t_1^*/2) . \tag{21}$$

Thus the $\Delta\bar{v}$ cost is a linear function of the z-amplitude, indicating that larger orbits will incur more cost per revolution.

Higher Order Analysis with Z-Axis Control. In order to gain a better understanding of the $\Delta\bar{v}$ costs, and eventually produce a numerical path that includes the z-axis control strategy, it is necessary to approximate the path, including the $\Delta\bar{v}$'s, with the available analytic representations. To do so effectively, the linear z-axis control algorithm is extended for use with the higher order analytic approximations. The phase-plane plot of the third order solution (including eccentric primary orbits) appears circular. In actuality, however, it is slightly non-circular due to the higher order effects. If this slight change is regarded as small, as well as the coupling that occurs between the in-plane and out-of-plane motion for second and higher order terms, then the methodology of the linear analysis may be re-applied to produce a corresponding higher order algorithm for computing the $\Delta\bar{v}$'s. However, some significant changes are required and are specified below.

The approach used for the higher order analysis is an algorithmic one (as opposed to analytic, as determined for the linear analysis), and uses analytic solutions to provide higher order approximations for the path. For the descriptions that follow, the third order approximations are used (including eccentric primary orbits) unless otherwise stated. If amplitudes and phase angles are specified, the analytic solution provides a typical

Lissajous orbit, which will eventually pass through the excluded zone. The adopted strategy uses the phase angles given by Eq. (7) in order to prevent the spacecraft from entering the excluded zone for the longest possible time. For longer missions, z-axis control must then be integrated into this orbit in some manner to prevent violation of the inner constraint.

To discuss the step-by-step analysis to incorporate this control strategy, it is necessary to note two complications when employing the higher order analytic approximations. First, when using the higher order approximations that include eccentricity, each revolution in the phase-plane plot is slightly different. Thus, a single desired near-circular path is not simply "repeated" a predetermined number of times. Rather, at a specific location along the Lissajous curve when the shape is near-circular, a path of one revolution duration is computed including two maneuvers that produce the circular shape. This revolution then (which is *not* a part of the natural Lissajous path), is identified as the nominal path to be maintained with z-axis control. However, since R changes with time, the general characteristics of this nominal revolution change slightly with each pass. This requires separate analysis of each revolution that uses the z-axis control plan (i.e., the nominal path varies slightly with each revolution). Also, each revolution must be analyzed in succession (*not* independently). Secondly, when using the analytic solution with eccentricity, the mean anomaly associated with the orbit of the primaries must be specified so that the relative locations of the primaries are known. The mean anomaly is determined through identification of three times: t_E, t_p, and t_R. Assume that the trajectory originates at time $t = 0$ (which can occur at any point along the path of the primaries). Let t_E be defined as the time at which the analytic solution is to be evaluated relative to the trajectory origin ($t = 0$). Then t_p is the time of periapsis passage of the primaries also relative to the trajectory origin. Finally, t_R is then the time since periapsis of the primaries along their path. Given t_E and t_p, it is determined as $t_R = t_E - t_p$. The time t_R, of course, corresponds to the mean anomaly from which R, the distance between the primaries, can be produced. The resulting R then corresponds to the evaluation time t_E. As an example, when the analytic solution is evaluated at time $t_E = 0$, the time that the primaries will be (or were) at periapsis is $t = t_p$. Thus, if $t_p = 100$ days, then the primaries will be at periapsis at time $t = 100$ days, so $t_R = -100$, i.e., the distance R is required to be the distance between the primaries at 100 days prior to periapsis. With these clarifications, discussion of the details of the procedure can proceed.

The algorithm that incorporates the control strategy approximates the path using the analytic representations available. A prior assessment results in identification of the specific location along the natural Lissajous path at which the initial uncontrolled portion of the trajectory has evolved into the desired near-circular shape. This point also identifies initiation of the controlled segment of the total trajectory. The algorithm then begins with selection of the specific point in time, defined as t_s, that will trigger implementation of the z-axis control strategy (t_s corresponds to some arbitrary point prior to the first "controlled" revolution of the nominal path). A search is then performed using the analytic solution for time $t > t_s$ until a time t_{max_1} is found such that the maximum z-excursion for that revolution occurs at t_{max_1}. The search resumes for $t > t_{max_1}$ until the following minimum z-value is found, and this time is defined t_{min_1}. The search continues again to the next maximum z-value, defined to occur at time t_{max_2}. For the i^{th} revolution (along the z-axis controlled portion of the trajectory), the "z" period is then computed as

$$\mathbf{P}_{z_i} = t^{(i)}_{max_2} - t^{(i)}_{max_1} \quad . \tag{22}$$

In a similar procedure, the i^{th} "xy" period $\mathbf{P}_{xy_i}$ is also computed. The difference in the two periods for the i^{th} revolution is then given by

$$\Delta P_i = P_{z_i} - P_{xy_i} \ . \tag{23}$$

Recalling that each controlled revolution of the nominal path is different and must be analyzed separately, it is important to note that t_s is re-used as the starting time for the searching procedure in the analytic solution, so that values obtained from the analytic solution will continue to correspond to the same specific location along a Lissajous curve. By re-using t_s, the times at which the analytic solution is evaluated (t_E) will no longer correspond to the actual time, since the time scale has been reset (and of course, the spacecraft continues its orbit in real time). However, it is necessary to compensate for the advance of the primaries along their respective paths. Thus, for other than the first revolution of the nominal path, the correct initial locations of the primaries will no longer be computed relative to the original value of t_p. A correction to t_p must be made since it is now further in the past. Let the original value of t_p be denoted by t_{p_o}. Since each controlled revolution along the nominal path has a duration of P_{xy_i}, the primaries can be placed in their correct initial locations by reducing t_{p_o} by the amount P_{xy_i} for each revolution. Thus for the searching procedure, the value of t_p to be used for analysis of the i^{th} controlled revolution is

$$t_{p_s}^{(i)} = t_{p_o} - \sum_{j=1}^{i-1} P_{xy_j} \ . \tag{24}$$

The difference between the two periods, ΔP_i, also varies with each controlled revolution. The magnitude of ΔP_i is an important quantity for the $\Delta\bar{v}$ calculation, as can be seen in Eqs. (19) and (21). Once ΔP_i has been found, the required $\Delta\bar{v}$'s for the i^{th} revolution can be obtained by using the phase-plane method described earlier. The linear analysis reduces the z-period P_{z_i} by using each $\Delta\bar{v}$ to trim or "skip" a time of length $\Delta P_i/2$ along the trajectory. Two $\Delta\bar{v}$'s per revolution then reduce the z-period the amount required to match the xy-period. The same concept is applied for the higher order analysis, defining the first $\Delta\bar{v}$ required during a revolution as

$$\Delta\bar{v}_i^1 = \dot{z}(t_{max_1}^{(i)} + \Delta P_i/4) - \dot{z}(t_{max_1}^{(i)} - \Delta P_i/4) \ , \tag{25}$$

where "i" denotes the "i^{th}" controlled revolution and the superscript "1" represents the first $\Delta\bar{v}$ during that revolution. The first term on the right-hand side of Eq. (25) represents the z component of the spacecraft velocity after the "jump" on the phase-plane plot. The second term is, of course, the z-velocity before the $\Delta\bar{v}_i^1$ is executed. Both values of the velocities are obtained from the analytic solution. As mentioned previously, evaluation of the primary distance R, through t_R, that corresponds to the evaluation time t_E requires adjustment since a portion of the original analytic trajectory is eliminated. The adjustment is again accomplished through t_p. For computing the z-velocity just before the maneuver, t_p is adjusted by the amount

$$t_{p_-}^{(i,1)} = t_{p_o} - \sum_{j=1}^{i-1} P_{xy_{j-1}} \ . \tag{26}$$

Similarly, t_p must be adjusted when computing the z-velocity just after $\Delta\bar{v}_i^1$ as

$$t_{p_+}^{(i,1)} = t_{p_o} + \Delta P_i/2 - \sum_{j=1}^{i-1} P_{xy_{j-1}} \ . \tag{27}$$

The term "$\Delta P_i/2$" includes the duration of that portion of the path eliminated by the maneuver $\Delta\bar{v}_i^1$.

The second maneuver $\Delta\bar{v}_i^2$ is then found in a manner similar to $\Delta\bar{v}_i^1$ and computed as

$$\Delta\bar{v}_i^2 = \dot{z}(t_{min_1}^{(i)} + \Delta P_i/4) - \dot{z}(t_{min_1}^{(i)} - \Delta P_i/4) \quad . \tag{28}$$

As before, the value of t_p must be adjusted to account for the revolution number and for the trajectory arcs that are bypassed. When using the analytic solution to compute the z-velocity just before the second $\Delta\bar{v}$, t_p is adjusted to

$$t_{p_-}^{(i,2)} = t_{p_o} + \Delta P_i/2 - \sum_{j=1}^{i-1} P_{xy_{j-1}} \quad , \tag{29}$$

and for $\dot{z}$ just after $\Delta\bar{v}_i^2$,

$$t_{p_+}^{(i,2)} = t_{p_o} + \Delta P_i - \sum_{j=1}^{i-1} P_{xy_{j-1}} \quad . \tag{30}$$

The above procedure is repeated for the desired number of controlled revolutions, and the total $\Delta\bar{v}$ cost is calculated as

$$\Delta\bar{v}_{tot} = \sum_{i=1}^{N} (\mid \Delta\bar{v}_i^1 \mid + \mid \Delta\bar{v}_i^2 \mid) \quad , \tag{31}$$

where N is the number of controlled revolutions.

Numerical Solutions Using Z-Axis Control. As mentioned earlier, references 3 and 4 discuss a technique for the numerical determination of Lissajous trajectories in the elliptic restricted three-body problem. However, no provisions are made for accommodating the z-axis control plan in the method. In order to accomplish this, the z-axis control algorithm is used with an analytic approximation to provide an initial guess for the orbit. The numerical algorithm using the approach by Howell and Pernicka for computing Lissajous trajectories requires the guess in the form of target points spaced along the trajectory (typically at every half revolution), with each target point defined in terms of the appropriate position and velocity states. An algorithm has been developed that uses z-axis control and the analytic solution to compute and record these target states. (Details of this algorithm are given in reference 5). These targets can then be used in the numerical approach to compute a Lissajous trajectory that includes an arbitrary, predetermined number of controlled revolutions.

The algorithm used to construct the target states can be summarized as follows. First, the complete trajectory is divided into three segments. Initially, the spacecraft moves naturally along its Lissajous trajectory, and this is defined as Segment 1. When the path becomes approximately circular in shape, the z-axis control strategy is implemented. (Note that t_s is defined in the last revolution of Segment 1.) This part of the trajectory, that includes all of the design maneuvers needed to maintain the circular-type motion, is termed Segment 2. Finally, z-axis control is discontinued and the vehicle proceeds along its uninterrupted Lissajous path, and will eventually enter the exclusion zone. This portion of the trajectory is defined as Segment 3. The algorithm is thus most easily understood if it is divided into three separate parts corresponding to the trajectory sections defined above.

The method for computing the target states for Segment 1 is straightforward and independent of the z-axis control plan. An analytic solution is evaluated at time $t = 0$ in order to provide the position and velocity corresponding to the initial target state. Succeeding target states are obtained by evaluating the analytic solution at time increments corresponding to spacings of half or quarter revolutions along the trajectory. This procedure continues until the predetermined end of Segment 1 is reached.

The initial point of Segment 2 marks the location along the orbit path at which the z-axis control plan is activated (i.e., t_s). Target states are again defined at half or quarter revolutions along the trajectory. The algorithm uses Eqs. (25) and (28) to compute the $\Delta\bar{v}$'s such that each is located at a position that corresponds to a target state. The analytic solution is used to determine the target states, but some complications arise since the $\Delta\bar{v}$'s affect the time at which the analytic solution must be evaluated to provide the correct states. Reference 5 gives a detailed procedure for dealing with these complications.

Segment 3 is the final portion of the orbit, where once again the spacecraft returns to its natural trajectory. The target states for this segment are obtained in a procedure similar to that used for Segment 1.

Once the series of target states is available, the software for numerically computing Lissajous trajectories can then be used to obtain a continuous path. The target states are used as inputs to the algorithm. Also input are the $\Delta\bar{v}$'s produced by the higher order analysis for Segment 2 of the orbit. Recall that the numerical method for determination of the Lissajous trajectory involves an iterative procedure which reduces the velocity discontinuities at each target point to essentially zero. Now, the algorithm is modified such that, when z-axis control is used, the iterative procedure converges with the velocity discontinuities at the target points in Segment 2 equal to the values predicted by the higher order analysis. Since the velocity discontinuities are inputs to the algorithm, they can be set to any desired value. In some cases, a reduction in the total $\Delta\bar{v}$ cost has been achieved by "manually" lowering the magnitudes of the predicted maneuvers as produced in the higher order analysis. Components of each $\Delta\bar{v}$ can be adjusted individually. Continuing studies of this problem include investigation of the orbit sensitivity to change in the $\Delta\bar{v}$'s. Some additional constraints can also be accommodated. For example, a possible SOHO mission constraint would require maneuvers to be perpendicular to the the Sun-spacecraft line. Using the same technique previously outlined, small components of $\Delta\bar{v}$ can be used in the $\hat{x}$ and $\hat{y}$ directions in order to meet this constraint. (Such a requirement has had a negligible effect on total mission maneuver cost.)

Fig. 5 shows an example of a total Lissajous orbit that includes use of z-axis control over five revolutions to produce a trajectory that does not violate the exclusion zone constraint during its specified duration of approximately six years. This trajectory uses the same input amplitudes and phase angles as the example shown in Fig. 1, and includes Segments 1, 2, and 3 as described previously. The orbit has an actual duration of 6.16 years, and a maneuver cost of 62.5 met/sec. (The maneuver cost is expended entirely in Segment 2.) The duration of the individual segments is as follows: Segment 1, 2.13 years; Segment 2, 2.16 years; and Segment 3, 1.87 years. The SEM model was used to compute this example, and the trajectory proceeds in a counter-clockwise direction. Numerous additional trajectories of various sizes have been produced. This includes trajectories that are controlled over their entire length to maintain a near-circular shape throughout the mission lifetime. In all cases examined, the fundamental approach has been successful in producing a trajectory. Additional studies will include trajectories with very large out-of-plane amplitudes for which the analytic approximation to the solution breaks down. Further development of the method and extension of its applicability is continuing.

CONCLUSION

A method for the numerical determination of Lissajous trajectories that includes a z-axis control strategy for avoiding an exclusion zone has been demonstrated. The example shown here was computed for a specific μ, however, the approach is quite general and

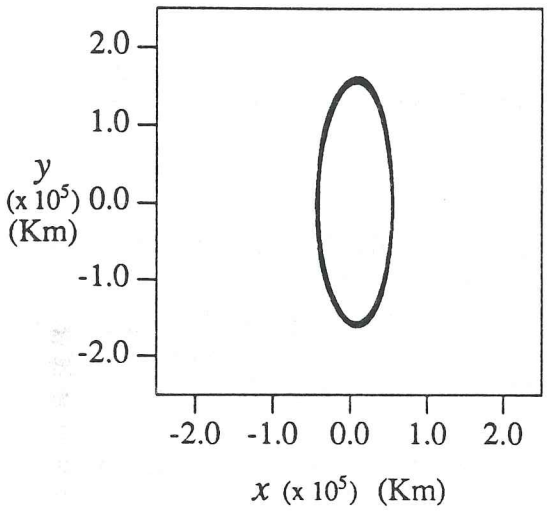

6.69 Year Trajectory

A_y = 157,000 km

A_z = 157,000 km

$\phi = 14.9^o$

$\psi = -26.4^o$

Maneuver Cost = 62.5 met/sec

(5 controlled revolutions
= 10 $\Delta\bar{v}$'s)

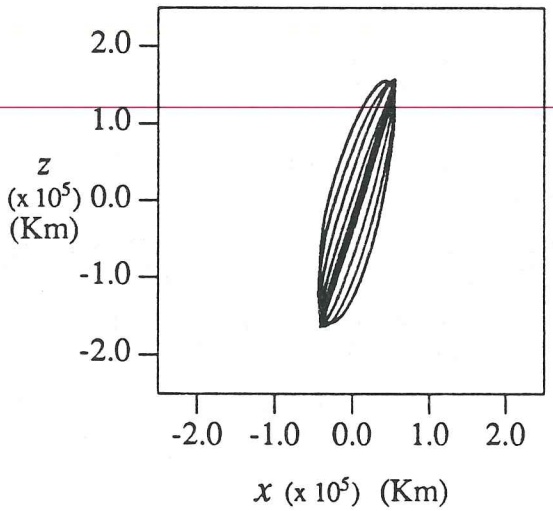

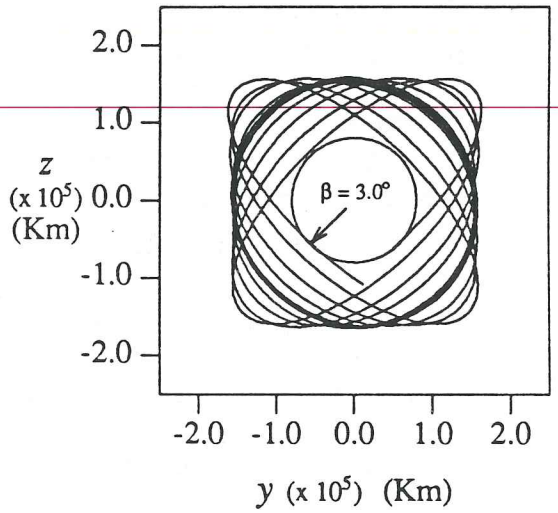

Fig. 5 Example Trajectory Using Z-Axis Control

will apply to a wide range of primary systems. The method also applies to either libration point L_1 or L_2. Future efforts may involve investigating techniques to further reduce the $\Delta\bar{v}$ cost required to satisfy the exclusion zone constraint.

ACKNOWLEDGEMENT

Portions of this work have been supported by the National Aeronautics and Space Administration under Grant No. NGT-50053, and by Computer Sciences Corporation.

REFERENCES

1. R.W. Farquhar and A.A. Kamel, "Quasi-Periodic Orbits About the Translunar Libration Point," *Celestial Mechanics,* Vol. 7, 1973, pp. 458-473.

2. D.L. Richardson and N.D. Cary, "A Uniformly Valid Solution for Motion About the Interior Libration Point of the Perturbed Elliptic-Restricted Problem," *AAS/AIAA Astrodynamics Specialists Conference,* Nassau, Bahamas, July 28-30, 1975, AAS Paper 75-021.

3. K.C. Howell and H.J. Pernicka, "Numerical Determination of Lissajous Trajectories in the Restricted Three-Body Problem," *Celestial Mechanics,* Vol. 41, 1988, pp. 107-124.

4. K.C. Howell, "Trajectory Design for Libration Point Trajectories and for Double Lunar Swingby Trajectories," Final Report prepared for Computer Sciences Corporation, December 1987.

5. K.C. Howell, "Design of Libration Point Trajectories and Consecutive Lunar Encounter Trajectories," Final Report prepared for Computer Sciences Corporation, September 1988.

6. R.W. Farquhar, "The Moon's Influence on the Location of the Sun-Earth Exterior Libration Point," *Celestial Mechanics,* Vol. 2, 1970, pp. 131-133.

7. J.D. Porter, "Final Report for Lunar Libration Point Flight Dynamics Study," NASA GSFC Contract NAS-5-11551, April 1969, General Electric Co., Philadelphia, Pa.

8. R.W. Farquhar, "Lunar Communications with Libration-Point Satellites," *Journal of Spacecraft and Rockets,* Vol. 4, No. 10, October 1967, pp. 1383-1384.

9. R.W. Farquhar, "Station-keeping in the Vicinity of Collinear Libration Points with an Application to a Lunar Communications Problem," *Space Flight Mechanics,* Science and Technology Series, American Astronautical Society, New York, 1967, Vol. 11, pp. 519-535.

10. R.W. Farquhar, "Comments on 'Optimal Controls for Out-of-Plane Motion about the Translunar Libration Point,' " *Journal of Spacecraft and Rockets,* Vol. 8, No. 7, July 1971, pp. 815-816.

11. T.A. Heppenheimer, "Optimal Controls for Out-of-Plane Motion about the Translunar Libration Point," *Journal of Spacecraft and Rockets,* Vol. 7, No. 9, September 1970, pp. 1087-1092.